Cascaded Raman lasing in packaged high quality As_2S_3 microspheres

Francis Vanier,[1,*] **Yves-Alain Peter**[1] **and Martin Rochette**[2]

[1]*Department of Engineering Physics, Polytechnique Montréal, Montréal (QC), H3C 3A7 Canada*

[2]*Department of Electrical and Computer Engineering, McGill University, Montréal (QC), H3A 2A7 Canada*

[*]*francis-2.vanier@polymtl.ca*

Abstract: We report the observation of cascaded Raman lasing in high-Q As_2S_3 microspheres. Cascaded stimulated Raman scattering emission is obtained up to the 5^{th} order for a pump wavelength of 1557 nm and up to the 3^{rd} order for a pump wavelength of 1880 nm. High-Q As_2S_3 microspheres are used in a self-frequency locking laser setup without an external laser source. Threshold curves measurements are presented and follow the expected coupled mode theory behavior with a sub-mW threshold pump power.

OCIS codes: (140.3945) Microcavities; (160.4330) Nonlinear optical materials; (140.3550) Lasers, Raman; (190.5650) Raman effect.

References and links

1. M. Asobe, T. Kanamori, K. Naganuma, H. Itoh, and T. Kaino, "Third-order nonlinear spectroscopy in As_2S_3 chalcogenide glass fibers," J. App. Phys. **77**(11), 5518–5523 (1995).
2. R. E. Slusher, G. Lenz, J. Hodelin, J. Sanghera, L. B. Shaw, and I. D. Aggarwal, "Large Raman gain and nonlinear phase shifts in high-purity As_2Se_3 chalcogenide fibers," J. Opt. Soc. Am. B **21**(6), 1146–1155 (2004).
3. S. D. Jackson and G. Anzueto-Sánchez, "Chalcogenide glass Raman fiber laser," Appl. Phys. Lett. **88**, 221106 (2006).
4. O. P. Kulkarni, C. Xia, D. J. Lee, M. Kumar, A. Kuditcher, M. N. Islam, F. L. Terry Jr., M. J. Freeman, B. G. Aitken, S. C. Currie, J. E. McCarthy, M. L. Powley, and D. A. Nolan, "Third order cascaded Raman wavelength shifting in chalcogenide fibers and determination of Raman gain coefficient," Opt. Express **14**(17), 7924–7930 (2006).
5. C. Xiong, E. Magi, F. Luan, A. Tuniz, S. Dekker, J. S. Sanghera, L. B. Shaw, I. D. Aggarwal, and B. J. Eggleton, "Characterization of picosecond pulse nonlinear propagation in chalcogenide As_2S_3 fiber," Appl. Opt. **48**(29), 5467–5474 (2009).
6. N. Ducros, F. Morin, K. Cook, A. Labruyère, S. Février, G. Humbert, F. Druon, M. Hanna, P. Georges, J. Canning, R. Buczynski, D. Pysz, and R. Stepien, "Frequency conversion from near-infrared to mid-infrared in highly nonlinear optical fibres," Proc. SPIE **7714**, 77140B (2010).
7. R. T. White and T. M. Monro, "Cascaded Raman shifting of high-peak-power nanosecond pulses in As_2S_3 and As_2Se_3 optical fibers," Opt. Lett. **36**(12), 2351–2353 (2011).
8. M. Duhant, W. Renard, G. Canat, T. N. Nguyen, F. Smektala, J. Troles, Q. Coulombier, P. Toupin, L. Brilland, P. Bourdon, and G. Renversez, "Fourth-order cascaded Raman shift in AsSe chalcogenide suspended-core fiber pumped at 2 μm," Opt. Lett. **36**(15), 2859–2861 (2011).
9. R. Ahmad and M. Rochette, "Chalcogenide microwire based Raman laser," Appl. Phys. Lett. **101**, 101110 (2012).
10. R. Ahmad and M. Rochette, "Raman lasing in a chalcogenide microwire-based Fabry-Perot cavity," Opt. Lett. **37**(21), 4549–4551 (2012).
11. M. Bernier, V. Fortin, N. Caron, M. El-Amraoui, Y. Messaddeq, and R. Vallée, "Mid-infrared chalcogenide glass Raman fiber laser," Opt. Lett. **38**(2), 127–129 (2013).
12. M. Bernier, V. Fortin, M. El-Amraoui, Y. Messaddeq, and R. Vallée, "3.77 μm fiber laser based on cascaded Raman gain in a chalcogenide glass fiber," Opt. Lett. **39**(7), 2052–2055 (2014).

#224127 - $15.00 USD Received 2 Oct 2014; revised 31 Oct 2014; accepted 1 Nov 2014; published 10 Nov 2014

13. S. M. Spillane, T. J. Kippenberg, and K. J. Vahala, "Ultralow-threshold Raman laser using a spherical dielectric microcavity," Nature (London) **415**, 621–623 (2002).
14. B. Min, T. J. Kippenberg, and K. J. Vahala, "Compact, fiber-compatible, cascaded Raman laser," Opt. Lett. **28**(17), 1507–1509 (2003).
15. T. J. Kippenberg, S. M. Spillane, D. K. Armani, and K. J. Vahala, "Ultralow-threshold microcavity Raman laser on a microelectronic chip," Opt. Lett. **29**(11), 1224–1226 (2004).
16. I. S. Grudinin and L. Maleki, "Ultralow-threshold Raman lasing with CaF_2 resonators," Opt. Lett. **32**(2), 166–168 (2007).
17. J. Moore, M. Tomes, T. Carmon, and M. Jarrahi, "Continuous-wave cascaded-harmonic generation and multi-photon Raman lasing in lithium niobate whispering-gallery resonators," Appl. Phys. Lett. **99**, 221111 (2011).
18. J. Hu, N. Carlie, L. Petit, A. Agarwal, K. Richardson, and L. Kimerling, "Demonstration of chalcogenide glass racetrack microresonators," Opt. Lett. **33**(8), 761–763 (2008).
19. M. E. Solmaz, D. B. Adams, W. C. Tan, W. T. Snider, and C. K. Madsen, "Vertically integrated As_2S_3 ring resonator on $LiNbO_3$," Opt. Lett. **34**(11), 1735–1737 (2009).
20. L. Li, H. Lin, S. Qiao, Y. Zou, S. Danto, K. Richardson, J. D. Musgraves, N. Lu, and J. Hu, "Integrated flexible chalcogenide glass photonic devices," Nat. Photonics **8**, 643–649 (2014).
21. J. Hu, N. Carlie, N.-N. Feng, L. Petit, A. Agarwal, K. Richardson, and L. Kimerling, "Planar waveguide-coupled, high-index-contrast, high-Q resonators in chalcogenide glass for sensing," Opt. Lett. **33**(21), 2500–2502 (2008).
22. H. Lin, L. Li, Y. Zou, S. Danto, J. D. Musgraves, K. Richardson, S. Kozacik, M. Murakowski, D. Prather, P. T. Lin, V. Singh, A. Agarwal, L. C. Kimerling, and J. Hu, "Demonstration of high-Q mid-infrared chalcogenide glass-on-silicon resonators," Opt. Lett. **38**(9), 1470–1472 (2013).
23. F. Luan, E. Magi, T. Gong, I. Kabakova, and B. J. Eggleton, "Photoinduced whispering gallery mode microcavity resonator in a chalcogenide microfiber," Opt. Lett. **36**(24), 4761–4763 (2011).
24. G. R. Elliott, D. W. Hewak, G. Senthil Murugan, and J. S. Wilkinson, "Chalcogenide glass microspheres; their production, characterization and potential," Opt. Express **15**(26), 17542–17553 (2007).
25. C. Grillet, S. N. Bian, E. C. Magi, and B. J. Eggleton, "Fiber taper coupling to chalcogenide microsphere modes," Appl. Phys. Lett. **92**, 171109 (2008).
26. D. H. Broaddus, M. A. Foster, I. H. Agha, J. T. Robinson, M. Lipson, and A. L. Gaeta, "Silicon-waveguide-coupled high-Q chalcogenide microspheres," Opt. Express **17**(8), 5998–6003 (2009).
27. G. R. Elliott, G. Senthil Murugan, J. S. Wilkinson, M. N. Zervas, and D. W. Hewak, "Chalcogenide glass microsphere laser," Opt. Express **18**(25), 26720–26727 (2010).
28. P. Wang, G. Senthil Murugan, G. Brambilla, M. Ding, Y. Semenova, Q. Wu, and G. Farrell, "Chalcogenide microsphere fabricated from fiber tapers using contact with a high-temperature ceramic surface," IEEE Photonics Technol. Lett. **24** (13), 1103–1105 (2012).
29. P. Wang, M. Ding, T. Lee, G. Senthil Murugan, L. Bo, Y. Semenova, Q. Wu, D. Hewak, G. Brambilla, and G. Farrell, "Packaged chalcogenide microsphere resonator with high Q-factor," Appl. Phys. Lett. **102**, 131110 (2013).
30. F. Vanier, M. Rochette, N. Godbout, and Y.-A. Peter, "Raman lasing in As_2S_3 high-Q whispering gallery mode resonators," Opt. Lett. **38**(23), 4966–4969 (2013).
31. O. Aktas, E. Ozgur, O. Tobail, M. Kanik, E. Huseyinoglu, and M. Bayindir, "A new route for fabricating on-chip chalcogenide microcavity resonator arrays," Adv. Optical Mater. **2**(7), 618–625 (2014).
32. K. Kieu and M. Mansuripur, "Fiber laser using a microsphere resonator as a feedback element," Opt. Lett. **32**(3), 244–246 (2007).
33. A. Schulte, C. Rivero, K. Richardson, K. Turcotte, V. Hamel, A. Villeneuve, T. Galstian, and R. Vallée, "Bulk-film structural differences of chalcogenide glasses probed in situ by near-infrared waveguide Raman spectroscopy," Opt. Commun. **198**(1-3), 125–128 (2001).

1. Introduction

Stimulated Raman scattering (SRS) and cascaded SRS are important nonlinear optical phenomena for signal generation at wavelengths that are not accessible by conventional semiconductor and rare-earth doped sources. This is due to the fact that Raman gain is available over the entire transparency window of the host material. This can be especially important for the $2-12\ \mu$m mid-IR region for molecular spectroscopy and biosensing applications.

Chalcogenide glasses such as As_2S_3 are ideal materials in this regard as they provide a wide transparency window over the mid-IR. Widespread under the form of high purity fibers, chalcogenide glasses are also known for their high Raman gain typically more than 100 times the gain of silica [1, 2]. SRS and cascaded SRS processes were already observed in As_2S_3 and As_2Se_3 fibers, tapered fibers and suspended core fibers [2–12].

Whispering gallery modes (WGM) microcavities such as spheres, disks and toroids are ex-

#224127 - $15.00 USD Received 2 Oct 2014; revised 31 Oct 2014; accepted 1 Nov 2014; published 10 Nov 2014

cellent structures for SRS emission thanks to their high Q-factors and small modal volumes. SRS and cascaded SRS emission were also demonstrated in silica spheres and toroids, CaF_2 disks and $LiNbO_3$ disks [13–17]. Typical input power threshold $< 100\ \mu$W were obtained for the first Raman order emission due to the cavity high Q-factor $> 10^8$ [13, 16].

Chalcogenide WGM cavities such as As_2S_3 and $Ge_{23}Sb_7S_{70}$ racetracks [18–20], As_2S_3 and As_2Se_3 disks [21, 22], As_2S_3 microfibers [23] and Ga:La:S, As_2S_3 and As_2Se_3 spheres [24–31] were also fabricated. Despite the high potential of chalcogenide glasses as a SRS medium, it was not until recently that SRS emission was observed in chalcogenide WGM cavities. First order SRS emission with a threshold pump power of 35 μW was shown in As_2S_3 microspheres with a Q-factor of 7×10^7 [30].

In this article, we demonstrate cascaded SRS emission in As_2S_3 high-Q microspheres up to the 5^{th} Raman order pumped at a wavelength of 1557 nm. Threshold power measurements show the expected coupled mode theory dynamics for the first three Raman order emission. A laser pumping setup without an external source is presented together with a packaging technique for the microsphere and the tapered fiber. Testing was also performed using a pump wavelength of 1880 nm. SRS emission up to the 3^{rd} order was obtained at a wavelength of 2350 nm. These results show the potentiel of As_2S_3 high-Q microspheres to act as sub-mW pump power cascaded SRS sources in the telecommunication band and in the $2-6\ \mu$m mid-IR range.

2. Self-frequency locking laser setup

Chalcogenide glasses such as As_2S_3 have a relatively high thermorefractive coefficient $\frac{dn}{dT}$. This property makes it difficult to couple an external signal to a high-Q optical mode because the resonance rapidly shifts away as the mode region heats up, and limits the optical power coupled inside the cavity. To mitigate this behavior, we used a self-frequency locking laser setup shown Fig. 1 [32]. The amplified signal of an Er-doped fiber amplifier (EDFA) is sent through a tunable band-pass filter (TBF) with a bandwidth of 0.2 nm and tunable throughout the telecommunication C-band. An isolator (Iso) prevents any back-reflection to be amplified and ensures the signal direction in the fiber cavity. The filtered optical signal goes through a circulator and is evanescently coupled to an As_2S_3 microsphere using a silica tapered fiber with a diameter of 2 μm. The microspheres are fabricated from reshaping the tip of a fine As_2S_3 wire using a CO_2 laser. The Q-factors of the spheres typically reach 10^7 [30]. Some high-Q resonances act as narrow band mirror when they are mode-splitted by a small perturbation such as surface roughness or a dust particle. A single laser line is typically reflected back in the fiber cavity. The bandwidth of a high-Q resonance is usually below 1 pm at a wavelength

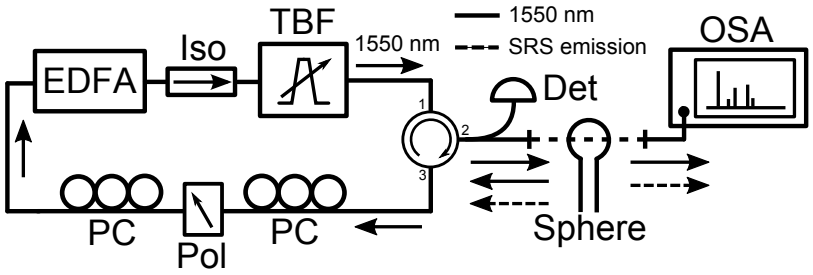

Fig. 1. Self-frequency locking laser setup - The gain signal from a Er-doped fiber amplifer is filtered using a 0.2 nm bandwidth tunable band-pass filter. An As_2S_3 microsphere acts as a narrow-band mirror and sends back a single line emission in the fiber loop. The transmitted pump signal and the forward Raman signal is measured by the OSA. A powermeter measures the injected pump power in the tapered fiber.

#224127 - $15.00 USD Received 2 Oct 2014; revised 31 Oct 2014; accepted 1 Nov 2014; published 10 Nov 2014

of 1550 nm. The polarization controllers (PCs) and a polarizer (Pol) are used to optimize the coupling conditions to the microsphere. When the pump signal power is strong enough, SRS emission builds-up in the microsphere. The emitting pump signal and forward Raman signal are measured using a Yokogawa AQ6375 optical spectrum analyzer (OSA). The optical power sent to the microsphere is measured using an optical powermeter (Det). In this configuration, the signal is forced to propagate inside a high-Q mode of the microcavity and the lasing frequency is determined by the resonances of the microcavity.

3. Sphere encapsulation

Dust particles on the sphere surface increase the scattering losses and thus decrease the Q-factor. To avoid such detrimental contamination, the microsphere and the tapered silica fiber are packaged in a closed glass tube. Figure 2 shows the glass tube packaging process. First, glass half-rods are glued inside of the lower half of a 6 cm long glass tube with a low-expansion UV-polymer (Fig. 2(a)). The tapered silica fiber is fabricated and is glued on the half-rods (Fig. 2(b)). The fiber tip of the microsphere is then attached to the glass tube once the coupling condition and the transmission spectrum are optimized. Finally, the upper half of the glass tube is placed on top to complete the assembly (Fig. 2(c)). An image of a typical As_2S_3 high-Q microsphere is presented in Fig. 3(a).

It was recently shown that an As_2S_3 microsphere and a silica tapered fiber can be packaged in a UV-curable polymer [29]. Unfortunately, the additional loss caused by the polymer touching the sphere reduces the Q-factor of the sphere. Q-factors up to 2×10^5 were measured using this method.

In contrast, the glass tube packaging method leaves the tapered fiber and the microsphere suspended in air. The transmission of the tapered fiber and the high Q-factor of the sphere are not affected by this method. Resonances with a loaded Q-factor Q_L up to 10^7 are measured at a wavelength of 1550 nm after the packaging process. A high-Q resonance transmission spectrum is shown in Fig. 3(b) for a sphere with a diameter of 40 μm. Once sealed, the glass tube could be used as a gas chamber for gas sensing measurements if a mid-IR source were to be used.

4. Cascaded SRS emission from the 1550 nm wavelength region

Cascaded SRS emission is obtained when the gain provided by the previous Raman orders exceeds the losses of the present Raman order. Whispering gallery modes of cavities such as microspheres are ideal for cascaded SRS emission since they present high Q-factors, small

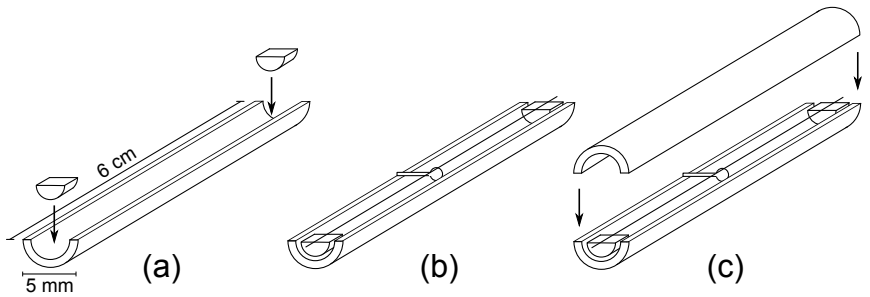

Fig. 2. Glass tube packaging - (a) Glass half-rods are installed in the lower half of a glass tube. (b) The tapered fiber is attached to the glass half-rods. While the microsphere is in a optimal coupling condition, its fiber tip is glued to the side of the half-tube. (c) The upper half of the glass tube is placed on top.

#224127 - $15.00 USD Received 2 Oct 2014; revised 31 Oct 2014; accepted 1 Nov 2014; published 10 Nov 2014

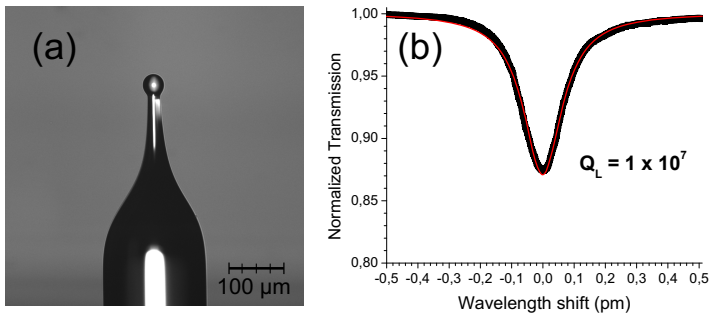

Fig. 3. (a) Image of a typical packaged As_2S_3 microsphere. (b) Transmission spectrum of a high-Q resonance from a packaged As_2S_3 microsphere. The loaded Q-factor $Q_L = 1 \times 10^7$.

mode volumes and a good mode overlap. A spectrum of the forward Raman signal power is presented in Fig. 4. The sphere used has a diameter of 50 μm and is in contact with the silica tapered fiber. SRS emission up to 5^{th} order is observed while pumping at a wavelength of 1557 nm and with a pump power of 6.3 mW. Raman emission peaks are located in multimode bands centered on wavelengths of 1646 nm, 1747 nm, 1861 nm, 1991 nm and 2140 nm respectively. The Raman shift of each successive Raman order corresponds to a value of ~ 10.5 THz. This value is in agreement with an in-house Raman spectroscopy measurement on the surface of our As_2S_3 spheres. A typical Raman spectroscopy measurement is shown in the inset of Fig. 4. This Raman shift for As_2S_3 was also predicted in [1, 33].

The SRS emission is multimode due to the large Raman gain bandwidth of As_2S_3 glass and the large number of high-Q cavity modes present across the spectrum. However, a single pump

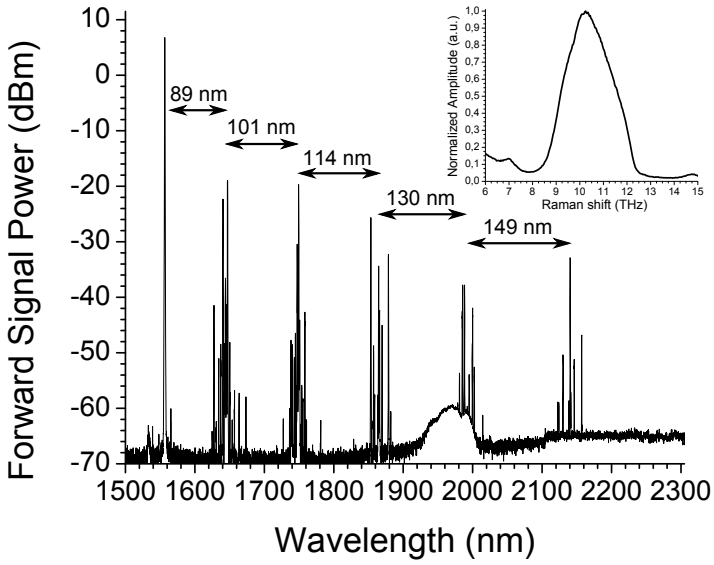

Fig. 4. Spectrum of a cascaded SRS emission of an As_2S_3 microsphere including 5 Raman orders generated from a pump wavelength of 1557 nm. The injected pump power in the tapered fiber is 6.3 mW. Each Raman order bands are centered on wavelengths of 1646 nm, 1747 nm, 1861 nm, 1991 nm and 2140 nm respectively. The inset shows a typical Raman spectroscopy measurement made on an As_2S_3 sphere surface.

#224127 - $15.00 USD Received 2 Oct 2014; revised 31 Oct 2014; accepted 1 Nov 2014; published 10 Nov 2014

mode contributes to the gain of all the first Raman order emission peaks. Each peak can then provide gain for the successive Raman order emission peaks. In this multimode regime, mode competition causes fluctuation of the output Raman power. To get a reliable power measurement, a regime where each Raman order emission is monomode is preferred.

Figure 5 shows the forward Raman signal power as a function of the injected pump power for three Raman orders. Each data point are extracted from a spectral measurement for different injected pump power values. The pump and the three Raman orders wavelengths are 1536 nm, 1619 nm, 1721 nm and 1830 nm respectively. In Fig. 5(a), as the pump power is increased, the first Raman order emission starts at an injected pump power of 370 μW and it follows a square root dependency as expected [14]. In the inset of Fig. 5(a), a square root curve fit shows that the first Raman order emission saturates at a pump power of ~ 450 μW. The saturation is caused by the SRS emission of a second Raman order presented in Fig. 5(b). The growth of the second order follows an expected linear dependency as the pump power increases. A linear curve fit indicates a threshold pump power of 430 μW. The first Raman order saturation is maintained until a pump power of ~ 600 μW where the first order emission increases again for a higher pump power. It coincides with the SRS emission of a third Raman order shown in Fig. 5(c). Again, the Raman signal power of the first and third order are in agreement with a square root tendency [14]. A square root curve fit shows a threshold pump power of 607 μW. The error on pump power measurement is limited by the fluctuation of the pump power circulating in the fiber cavity. The error on the forward Raman signal power is based on the noise level of the OSA.

The forward external efficiency $\eta_{ext} = dP_{Ri}/dP_{in}$, where P_{Ri} is the ith Raman order signal power and P_{in} is the injected pump power, are $(1.3 \pm 0.8) \times 10^{-2}$ %, $(1.23 \pm 0.02) \times 10^{-2}$ % and $(7 \pm 2) \times 10^{-3}$ % for the first, second and third Raman order respectively. These relatively low values are attibuted to a low coupling phase matching between the optical modes of the cavity and the silica tapered fiber, hence being in a undercoupling condition $Q_c >> Q_0$ with the coupling Q-factor Q_c and the intrinsic Q-factor Q_0. The use of an As_2S_3 tapered fiber would greatly increase the coupling coefficient and the Raman signal extraction.

5. Cascaded SRS emission from the 1880 nm wavelength region

An important property of As_2S_3 glass is its tranparency window across the $2-6$ μm spectral range. Combining this property, a high Raman gain and the high Q-factor of As_2S_3 microspheres could lead to low power mid-IR sources. To test this idea, we replaced the Er-doped fiber amplifier in Fig. 1 with a Tm-doped fiber amplifier to shift the Raman pump wavelength near 2 μm. The setup is shown in Fig. 6. A pump signal at a wavelength of 1550 nm is sent to a 32-cm long Tm-doped fiber. The gain signal in the 1800-1900 nm spectral region propagates to an As_2S_3 microsphere. Again, this setup uses the microsphere as a narrow band mirror. The reflected signal is sent back to the Tm-doped fiber. The isolator (Iso) forces the propagation direction. The polarization controller (PC) is used to optimize the coupling conditions and to select a preferred resonance group. The spectra are measured with an OSA.

In Fig. 7, a typical spectrum is presented for a multimode pump emission centered around a wavelength of 1880 nm. The signal power at a wavelength of 1550 nm that pumps the gain in the Tm-doped fiber is approximately 875 mW. The multimode 1880 nm pump signal in the microcavity leads to cascaded SRS emission up to the third order. The generated SRS signal is also multimode. SRS emission peaks are grouped around a wavelength of 2015 nm, 2170 nm and 2350 nm for the first, second and third order respectively. Again, the Raman shift is in agreement with the value of 10.3 THz.

These measurements show that As_2S_3 microspheres are good candidates for low power cascaded Raman sources. Furthermore, the transparency window of chalcogenide glasses such as

#224127 - $15.00 USD Received 2 Oct 2014; revised 31 Oct 2014; accepted 1 Nov 2014; published 10 Nov 2014

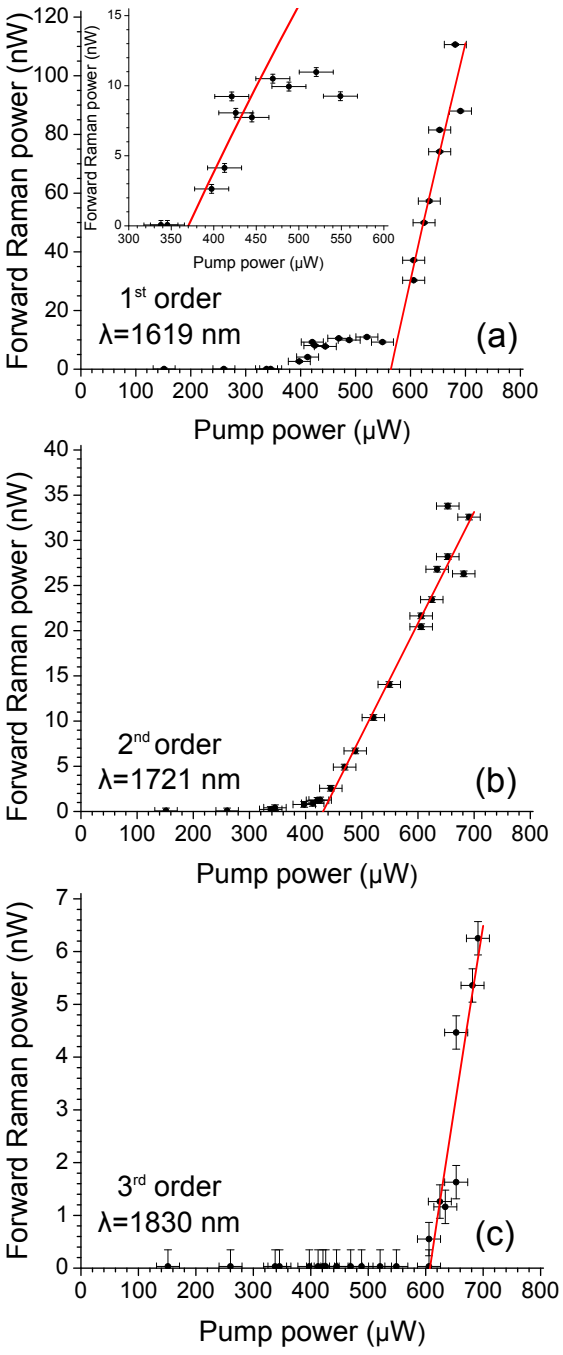

Fig. 5. Forward Raman signal power measurements for the (a) 1^{st} (b) 2^{nd} and (c) 3^{rd} Raman order. In the inset of (a), SRS threshold pump power is 370 μW. In (b), the threshold pump power of the second order Raman emission is 430 μW. The first order Raman signal saturates when the second order SRS emission power increases between 450 μW and 600 μW of pump power. In (c), the threshold power of the third Raman order is 607 μW. The first order Raman signal increases again when the third order Raman signal is getting stronger.

#224127 - $15.00 USD Received 2 Oct 2014; revised 31 Oct 2014; accepted 1 Nov 2014; published 10 Nov 2014

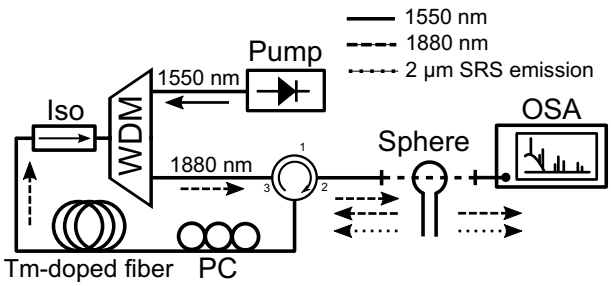

Fig. 6. Self-frequency locking laser setup at 1880 nm - The gain of a Tm-doped fiber is sent to the microsphere which acts as a narrow band mirror. The reflected signal is amplified in the fiber loop. The spectra are measured using an OSA.

As_2S_3 offers the possibility to extend the emission wavelength to the $2-6$ μm region. The As_2S_3 glass provided by CorActive High-Tech has an attenuation value below 1 dB/m across this spectral region. An upper Q-factor limit of 1×10^7 could be achieved if this attenuation value is considered. Provided that the laser fabrication technique produced microspheres with intrinsic Q-factors near this limit [30], the realisation of mid-IR As_2S_3 cascaded Raman sources with sub-mW of pump power seems possible.

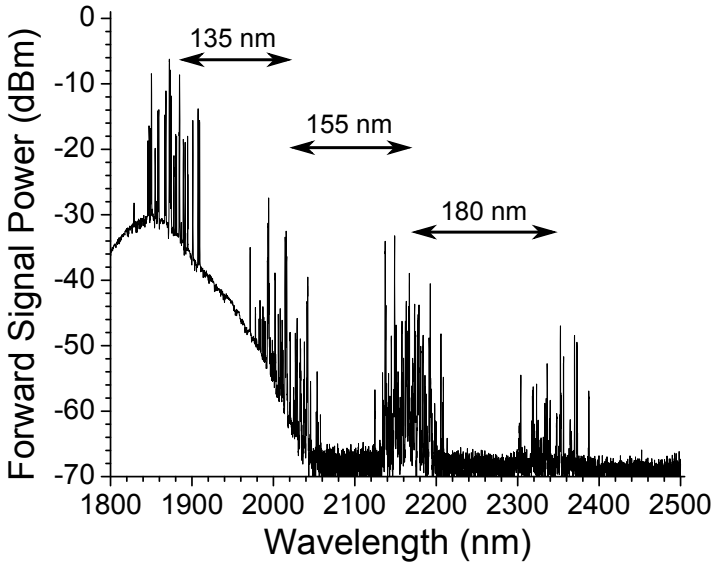

Fig. 7. Spectrum of a cascaded SRS emission with 3 Raman orders with a pump wavelength band centered on 1880 nm. Multimode Raman emission band positions are 2015 nm, 2170 nm and 2350 nm respectively.

6. Conclusion

In this work, we presented measurements of cascaded stimulated Raman scattering emission in As_2S_3 microspheres. Due to the high Raman gain of As_2S_3 and the high Q-factor resonances of the microspheres, SRS emissions up to the 5^{th} order were observed with a pump wavelength of 1557 nm. A self-frequency locking laser setup was used to mitigate the thermal drift of high Q-factor resonances. We introduced a packaging technique for an As_2S_3 sphere and a tapered

#224127 - $15.00 USD Received 2 Oct 2014; revised 31 Oct 2014; accepted 1 Nov 2014; published 10 Nov 2014

fiber which preserves the high Q-factors of the cavities. The measurements of the Raman signal power as a function of the input pump power were shown for the first three Raman orders. These measurements are in agreement with the expected theoretical behavior. Another setup was built to pump the microsphere at a wavelength of 1880 nm using a Tm-doped fiber amplifier. SRS emissions up to the 3^{rd} order were measured. These results reveal the potential of As_2S_3 microspheres as low power cascaded Raman sources at telecommunication wavelengths and in the $2-6$ μm mid-IR range.

Acknowledgments

The authors thank CorActive High-Tech for providing the As_2S_3 glass and the Tm-doped fiber used in this experiment. This work was supported by the Fonds de Recherche du Québec Nature et Technologies (FQRNT) Equipe grant 173906.

#224127 - $15.00 USD Received 2 Oct 2014; revised 31 Oct 2014; accepted 1 Nov 2014; published 10 Nov 2014